

# Three-body resonances in ${}^6\text{He}$ , ${}^6\text{Li}$ , and ${}^6\text{Be}$ , and the soft dipole mode problem of neutron halo nuclei

Attila Csóto\*

*W. K. Kellogg Radiation Laboratory, 106-38, California Institute of Technology, Pasadena, California 91125*  
(Received 12 January 1994)

Using the complex scaling method, the low-lying three-body resonances of  ${}^6\text{He}$ ,  ${}^6\text{Li}$ , and  ${}^6\text{Be}$  are investigated in a parameter-free microscopic three-cluster model. In  ${}^6\text{He}$  a  $2^+$ , in  ${}^6\text{Li}$  a  $2^+$  and a  $1^+$ , and in  ${}^6\text{Be}$  the  $0^+$  ground state and a  $2^+$  excited state is found. The other experimentally known  $2^+$  state of  ${}^6\text{Li}$  cannot be localized by our present method. We have found no indication for the existence of the predicted  $1^-$  soft dipole state in  ${}^6\text{He}$ . We argue that the sequential decay mode of  ${}^6\text{He}$  through the resonant states of its two-body subsystem can lead to peaks in the excitation function. This process can explain the experimental results in the case of  ${}^{11}\text{Li}$ , too. We propose an experimental analysis, which can decide between the soft dipole mode and the sequential decay mode.

PACS number(s): 21.10.-k, 21.60.Gx, 24.30.Gd, 27.20.+n

## I. INTRODUCTION

Recently, some experimental and theoretical analyses claimed the discovery of a new type of collective excitations, the soft dipole mode, in nuclei far from stability. It seems probable now, that in certain nuclei, near the neutron drip line, a dilute neutron halo with large spatial extension can exist around a compact core [1–5]; e.g., in  ${}^{11}\text{Li}$  and  ${}^6\text{He}$  two neutrons form the neutron halo around the  ${}^9\text{Li}$  and  ${}^4\text{He}$  cores, respectively. Shortly after their discovery it was predicted that the oscillation of the halo neutrons against the core can produce collective excited states in these nuclei [6]. These collective states are thought to be similar to the giant dipole resonances, where the neutrons of a nucleus oscillate against its protons. In the neutron halo nuclei the restoring force is weak (soft), which leads to low-frequency, viz. low-energy (1–5 MeV) states compared to the giant dipole resonances ( $\sim 20$  MeV).

The overwhelming majority of the experimental and theoretical studies confirm the existence of these low-energy soft dipole modes. However, all these works without exception conclude for the existence of these states from the behavior of certain quantities (bound state ap-

proximated energies and electric dipole strengths [7], excitation cross sections [2,8–10], dipole sum rules [11], etc.) at real energies, i.e., they are all indirect evidences of the soft dipole mode, thus they are far from being unambiguous. For instance, recently we demonstrated [12] that the possibility of resonance+scattering-type asymptotic behaviors in a three-body system can lead to an apparent, resonancelike structure in the three-body continuum. To show up a direct proof for the existence of the soft dipole mode, we must find three-body resonant poles of the scattering matrix at complex energies with the predicted properties (excitation energy, decay width, spin-parity).

In this paper we search for three-body resonances in  ${}^6\text{He}$  using the complex scaling method. In order to test our method, we study the  ${}^6\text{Li}$  and  ${}^6\text{Be}$  nuclei, as well.

## II. MODEL

Our model is a microscopic three-cluster ( $\alpha + N + N$ ) Resonating Group Method (RGM) approach to the six-nucleon systems. The trial function of the six-body problem has the form

$$\Psi = \sum_{(i,j,k)} \sum_{S,l_1,l_2,L} \mathcal{A} \left\{ \left[ [\Phi^i(\Phi^j\Phi^k)]_S \chi_{[l_1 l_2]L}^{i(jk)}(\rho_1, \rho_2) \right]_{JM} \right\}, \quad (1)$$

\*Electronic address: H988CSO@HUELLA.BITNET On leave from the Institute of Nuclear Research of the Hungarian Academy of Sciences, P.O. Box 51, Debrecen, H-4001, Hungary.

where the  $i, j$ , and  $k$  indices denote any one of the labels  $\alpha, n$ , and  $p$ , and the first sum runs over all possible different arrangements of the clusters  $[\alpha(nn)$  and  $n(\alpha n)$  in the case of  ${}^6\text{He}$ ,  $\alpha(pn)$ ,  $n(\alpha p)$ , and  $p(\alpha n)$  in the case of  ${}^6\text{Li}$ , and  $\alpha(pp)$  and  $p(\alpha p)$  in the case of  ${}^6\text{Be}$ ]. In (1)  $\mathcal{A}$  is the intercluster antisymmetrizer, the  $\Phi$  cluster internal states are translation invariant harmonic oscillator shell model states, the  $\rho$  vectors are the different intercluster Jacobi coordinates, and  $[\ ]$  denotes angular momentum coupling. In the sum over  $S, l_1, l_2$ , and  $L$  we should include all angular momentum configurations of any significance. Putting (1) into the six-nucleon Schrödinger equation we arrive at an equation for the intercluster relative motion functions  $\chi$ .

It is of prime importance to choose a nucleon-nucleon interaction which is appropriate for all subsystems appearing in the model space [13]. We choose the Minnesota interaction [14], containing central, Coulomb, and spin-orbit terms, with the parameters as in [13]. It was pointed out [13], that using the size parameter  $\beta = 0.606 \text{ fm}^{-2}$  for the  $\alpha$  particle, which minimizes its internal energy, together with the exchange mixture parameter  $u = 0.98$  of the Minnesota force, the experimental  $\alpha + N$  phase shifts can be excellently reproduced (see Fig. 1 of [13]). This force also gives very good phase shifts in the  ${}^1S_0$ , and  ${}^3P_J$  ( $J=0,1,2$ ) states of the  $n+n$  and  $p+p$  systems. Since our interaction cannot account for the charge independence breaking of the  $N-N$  force due to the different  $\pi^0$  and  $\pi^\pm$  pion masses, our  $p+n$  phase shifts are slightly worse than the  $n+n$  and  $p+p$  ones (see the discussion in [13]). It was emphasized in [13,15] that the Minnesota force is inappropriate in the  ${}^3S_1$   $N+N$  state, because it reproduces the ground state of the deuteron without the tensor coupling of the  ${}^3D_1$  state. This leads to a too strong interaction in the  ${}^3S_1$   $N+N$  state. Fortunately, in  ${}^6\text{He}$  and  ${}^6\text{Be}$  a triplet-even state cannot be present between the outer neutrons and protons, respectively, thus this problem does not appear. In  ${}^6\text{Li}$ , however, we have to pay definite attention to this problem. We neglect the tensor force because there is no firm ground to determine its parameters. For test purposes we shall use the tensor force of Refs. [16,17], which reproduces the  $J = 1, 2, 0$  order of the low-energy  ${}^3P_J$  phase shifts [13].

In a similar model [13] but using three size parameters for the  $\alpha$  (allowing two monopole excited states in addition to the ground state) and also including rearrangement (3+3 nucleon) channels, we got excellent results for the ground state of  ${}^6\text{He}$  and its (bound state approximated) isobar analogues in  ${}^6\text{Li}$  and  ${}^6\text{Be}$ . In that work we demonstrated that the high-lying 3+3 rearrangement channels are responsible for the 0.3–0.6 MeV energy lack appearing in the three-body models of the  $A = 6$  nuclei (for a recent review of the three-body models see [18], and the references therein). The  ${}^6\text{He}$  wave function of [13] was used in the study of the beta delayed deuteron emission from  ${}^6\text{He}$ , and proved to give good agreement with the experiment [15]. Unfortunately, the use of that huge model space would be hardly manageable computationally, and would cause numerical instabilities in the present work. Using only one size parameter for

the  $\alpha$  particle, and no rearrangements, we can keep the excellent reproduction of the  $\alpha + N$  phase shifts, which means that the description of the dynamics of the two-body subsystems is correct. The price we have to pay for this model space reduction is that the two-neutron separation energy in the ground state of  ${}^6\text{He}$  is not correct, being 0.670 MeV to be compared to the experimental value 0.975 MeV. We could get closer to the experiment including the  $t+t$  rearrangement channel. However, the inclusion of this channel into the  ${}^6\text{He}$  wave function requires the good reproduction of the  $\alpha + n$  phase shifts in a  $\{\alpha + n, t + d\}$  coupled channel model [13]. Although, using three  $\alpha$  size parameters we got excellent  $\alpha + n$  phase shifts in such a model [13], using only one  $\alpha$  size parameter it is no longer possible. The source of the problem is probably the change of the threshold splitting between the  $\alpha + n$  and  $d + t$  channels. We emphasize that requiring the good reproduction of the  $N + N$  and  $\alpha + N$  data, there is no remaining free parameter left in the model.

The next step is to find a method which can handle three-body resonances. There are indirect and direct ways of doing that. The indirect methods, e.g., [19], study the three-body problem at real energies, and extract resonance parameters from the three-body phase shifts. In the direct methods the aim is to find the complex energy poles of the three-body scattering matrix. For example, in [20–22] the authors determined the pole positions of the three-body  $S$  matrix by analytically continuing the homogeneous Faddeev equation to complex energies. To get a decisive answer to the question of the soft dipole mode of  ${}^6\text{He}$ , we must use a direct method. Our choice is the complex scaling method (CSM) [23]. This method reduces the problem of resonant states to that of bound states, and can handle the Coulomb interaction without any problem. It has been demonstrated recently that the CSM can be used to find three-body resonances in such problems which are very similar to our present situation [12]. Here we recall only the main points of the CSM, the details can be found in [12] and the references therein.

Suppose, we search for ( $N$ -body) resonant states of the Hamiltonian  $\hat{H}$ . We define a new Hamiltonian by

$$\hat{H}_\theta = \hat{U}(\theta)\hat{H}\hat{U}^{-1}(\theta), \quad (2)$$

where the  $\hat{U}(\theta)$  unbounded similarity transformation acts, in the coordinate space, on a function  $f(\mathbf{r})$  as

$$\hat{U}(\theta)f(\mathbf{r}) = e^{3i\theta/2}f(\mathbf{r}e^{i\theta}). \quad (3)$$

[If  $\theta$  is real,  $\hat{U}(\theta)$  means a rotation into the complex coordinate plane, if it is complex, it means a rotation and scaling.] In the case of a many-body Hamiltonian, (3) means that the transformation has to be performed in each Jacobi coordinate. If the potential is dilation analytic [24], then there is the following connection between the spectra of  $\hat{H}$  and  $\hat{H}_\theta$  [25]: (i) the bound eigenstates of  $\hat{H}$  are the eigenstates of  $\hat{H}_\theta$ , for any value of  $\theta$  within  $0 \leq \theta < \pi/2$ ; (ii) the continuous spectrum of  $\hat{H}$  will be rotated by an angle  $2\theta$ ; (iii) the complex gen-

erized eigenvalues of  $\widehat{H}_\theta$ ,  $\varepsilon_{\text{res}} = E - i\Gamma/2$ ,  $E, \Gamma > 0$  (where  $\Gamma$  is the full width at half maximum) belong to its proper spectrum, with square-integrable eigenfunctions, provided  $2\theta > |\arg \varepsilon_{\text{res}}|$ . In nuclear physics the CSM has been successfully applied in the RGM description of  ${}^8\text{Be}$  [26], in an Orthogonality Condition Model (OCM) of  ${}^{20}\text{Ne}$  [27], and in the OCM description of the resonances of  ${}^{10}\text{Li}$  [28].

Since the resonant wave functions become localized in the CSM, we can use any bound state method to describe them. Here we use an expansion of the wave function, in terms of products of tempered Gaussian functions of the Jacobi coordinates, in a variational method [13]. A typical term of this expansion looks like  $\rho_1^{l_1} \exp[-(\rho_1/\gamma_i)^2] Y_{l_1 m_1}(\widehat{\rho}_1) \cdot \rho_2^{l_2} \exp[-(\rho_2/\gamma_j)^2] Y_{l_2 m_2}(\widehat{\rho}_2)$ , where  $l_1$  and  $l_2$  are the angular momenta in the two relative motions, respectively, and the widths  $\gamma$  of the Gaussians are the parameters of the expansion. We choose ten  $\gamma$  parameters in each relative motion, and they follow a geometric progression [29] with  $\gamma_1 = 1$  fm and  $\gamma_{10} = 15$  fm.

### III. RESULTS

We have carried out calculations for the  $0^+$ ,  $1^+$ ,  $2^+$ ,  $0^-$ ,  $1^-$ , and  $2^-$  states in the  $A = 6$  nuclei. In order to keep all important angular momentum channels in Eq. (1), and at the same time keep the size of the problem manageable, we should know the contribution of each channel to the total wave functions. That is why we first made real energy calculations (i.e., without complex scaling) for the above-mentioned states, using square-integrable trial functions. The resulting weights of the different orthogonal  $(S, L)$  components are in Table I. The number of different  $\{i(jk); S, (l_1 l_2) L\}$  configurations in Eq. (1) was typically 10–12, most of them are nonorthogonal to each other. We calculated the amount of their clustering, which measure the weights of the different nonorthogonal channels [30,31,13], and kept the most important 5–6 channels in the complex calculations.

In  ${}^6\text{Li}$  we left out all angular momentum configuration which contain triplet-even state between the outer proton

and neutron. The inclusion of the configurations which contain the  ${}^3S_1$   $p + n$  state [e.g.,  $\{\alpha(pn); S, (l_1 l_2) L = 1, (02)2\}$  in the  $2^+$  state of  ${}^6\text{Li}$ ] would suppress all other channels because the Minnesota force is too strong in this  $p + n$  state. For example, this would lead to 99.8% weight of the  $(S, L) = (1, 2)$  component in the  $2^+$  state of  ${}^6\text{Li}$ , while without this  $\{\alpha(pn); 1, (02)2\}$  configuration the weight is only 0.5 %, as we can see in Table I. With their omission we dropped only a tiny part of the model space, because these components have large overlaps with the nonorthogonal angular momentum configurations in the  $(\alpha p)n$  and  $(\alpha n)p$  partitions [31]. Without a tensor force, the omission of the configurations which contain the  ${}^3D_1$   $p + n$  state almost does not change anything. If a tensor force and the  ${}^3D_1$   $p + n$  components [e.g., the  $\{\alpha(pn); 1, (20)2\}$  configuration in the  $1^+$  state of  ${}^6\text{Li}$ ] were present, the  ${}^6\text{Li}$  would become  $\sim 10$  MeV overbound. This is because our force would lead to a  $\sim 10$  MeV overbinding in the case of the  ${}^3S_1$ - ${}^3D_1$  coupled deuteron, itself. Although, we have no explicit  ${}^3S_1$   $p + n$  state in  ${}^6\text{Li}$ , the coupling of the  $\{\alpha(pn); 1, (20)2\}$  state to the  $(S, L) = (1, 0)$  channels, which are nonorthogonal to the omitted  $\{\alpha(pn); 1, (00)0\}$  component, would result in this  $\sim 10$  MeV overbinding of  ${}^6\text{Li}$ . With the omission of the triplet-even  $p + n$  components in  ${}^6\text{Li}$ , these problems do not appear, but the  $1^+$  ground state becomes slightly underbind ( $E = -3.01$  MeV compared to the experimental  $-3.70$  MeV). The  $3^+$  three-body bound state of  ${}^6\text{Li}$  appears at  $-1.77$  MeV (experiment:  $-1.51$  MeV). So, in conclusion, there is definitely room for improvements in  ${}^6\text{Li}$ . In the literature there are models for  ${}^6\text{Li}$ , e.g., [21], which do not suffer from the present force problem.

The parameters of all three-body resonances which we found are listed in Table II, along with the experimental energies and widths. We solved the complex scaled Schrödinger equations with different  $\theta$  rotation angles. Without approximations, the resulting pole position would not depend on  $\theta$ . Using an approximate method (in our case a variational method), the pole position slightly depends on  $\theta$ , and the stationary point of the  $\theta$  trajectory should be accepted as the position of the resonance [26]. Our best  $\theta$  values were around  $0.25$ – $0.3$  rad.

TABLE I. The weights (in percents) of the orthogonal  $(S, L)$  components in the various  $J^\pi$  states of  ${}^6\text{He}$ ,  ${}^6\text{Li}$ , and  ${}^6\text{Be}$ .

	$0^+$		$1^+$		$2^+$		$0^-$		$1^-$		$2^-$	
${}^6\text{He}$	(0,0)	86.5	(0,1)	0.5	(0,2)	52.8	(1,1)	100.0	(0,1)	86.0	(0,2)	<0.1
	(1,1)	13.5	(1,0)	2.0	(1,1)	46.5			(1,1)	14.0	(1,1)	100.0
			(1,1)	97.1	(1,2)	0.7			(1,2)	<0.1	(1,2)	<0.1
			(1,2)	0.4								
${}^6\text{Li}$	(0,0)	87.3	(0,1)	3.3	(0,2)	50.0	(1,1)	100.0	(0,1)	81.4	(0,2)	<0.1
	(1,1)	12.7	(1,0)	96.0	(1,1)	49.5			(1,1)	18.6	(1,1)	100.0
			(1,1)	0.7	(1,2)	0.5			(1,2)	<0.1	(1,2)	<0.1
			(1,2)	<sup>a</sup>								
${}^6\text{Be}$	(0,0)	87.7	(0,1)	0.2	(0,2)	59.9	(1,1)	100.0	(0,1)	84.0	(0,2)	<0.1
	(1,1)	12.3	(1,0)	0.6	(1,1)	39.6			(1,1)	16.0	(1,1)	100.0
			(1,1)	99.1	(1,2)	0.5			(1,2)	<0.1	(1,2)	<0.1
			(1,2)	0.1								

<sup>a</sup>Not included.

TABLE II. Energies (relative to the  $\alpha$  energy) and full widths of three-body resonances in  ${}^6\text{He}$ ,  ${}^6\text{Li}$ , and  ${}^6\text{Be}$ . The experimental values are taken from [32].

	$J^\pi(T)$	Theory		Experiment	
		$E$ (MeV)	$\Gamma$ (MeV)	$E$ (MeV)	$\Gamma$ (MeV)
${}^6\text{He}$	$2^+(1)$	0.74	0.06	$0.822 \pm 0.025$	$0.113 \pm 0.020$
${}^6\text{Li}$	$0^+(1)$	0.22	0.001	$-0.137^a$	
	$2^+(0)$		<sup>b</sup>	$0.610 \pm 0.022$	$1.7 \pm 0.2$
	$2^+(1)$	1.59	0.28	$1.696 \pm 0.015$	$0.54 \pm 0.020$
${}^6\text{Be}$	$1^+(0)$	5.71	3.89	$1.95 \pm 0.05$	$1.5 \pm 0.2$
	$0^+(1)$	1.52	0.16	$1.371 \pm^c$	$0.092 \pm 0.006$
	$2^+(1)$	2.81	0.87	$3.04 \pm 0.05$	$1.16 \pm 0.06$

<sup>a</sup>Bound state.

<sup>b</sup>Cannot be resolved by the present method (see the text).

<sup>c</sup>No errors are given in [32].

As a consequence of our not complete model space, which resulted in the  $\sim 10.7$  MeV underbinding in the ground state of  ${}^6\text{Li}$ , the  $1^+(T=0)$  resonance is pushed to higher energy, considerably increasing its width. The same underbinding effect which appeared in the ground state of  ${}^6\text{He}$  pushes the slightly bound  $0^+(T=1)$  state of  ${}^6\text{Li}$  into the continuum, resulting a three-body resonance. The experimentally known  $2^+(T=0)$  state of  ${}^6\text{Li}$  at  $E = 0.610$  MeV with  $\Gamma = 1.7$  MeV cannot be resolved by our present method because the pole at  $(0.610 - i0.85)$  MeV is mixed up with the points of the rotated discretized continuum, using any rotation parameter.

The agreement of the resonance parameters with the experimental values is good for the  $2^+(T=1)$  states of  ${}^6\text{He}$ ,  ${}^6\text{Li}$ , and  ${}^6\text{Be}$ , and the  $0^+$  state of  ${}^6\text{Be}$ . It is important to note that while our interaction underbinds the  $0^+$  state of  ${}^6\text{He}$  by about 0.3 MeV, the  $2^+$  state is "overbound" by about 0.1 MeV (and its width is smaller than the experimental value, accordingly). It means that the sometimes usual way to refit the interaction strength so as to get the correct binding energy for the ground state is dangerous. In our present case it would result in the parameters  $E = 0.46$  MeV and  $\Gamma = 0.008$  MeV for the  $2^+$  state. The best thing we can do is to accept the results, coming from an interaction which is good for the subsystems, as they are. To test the effect of the tensor interaction, we performed a calculation for the  $2^+$  state of  ${}^6\text{He}$  with the tensor force of [16,17] included. It resulted in  $E = 0.76$  MeV and  $\Gamma = 0.07$  MeV parameters, thus it has small effect.

The Riemann sheets, on which the resonances reside, can be uniquely identified by the relative position of the resonances and the rotated branch cuts [33,34].

To illustrate the working mechanism of our method, we show in Fig. 1 the results of the calculations for the  $2^+(T=1)$  and  $1^+(T=0)$  states in  ${}^6\text{Li}$ . As we can see, the rotated discretized continuum is a mixture of the three-body scattering continuum points, starting at the origin, and the resonance+scattering continua, starting at the  $3/2^-$  and  $1/2^-$  resonance positions of the  ${}^5\text{He}$  and  ${}^5\text{Li}$  subsystems [12]. The probably not accurate enough double-precision numerics and the interaction between the continua, which are close to each other, makes the

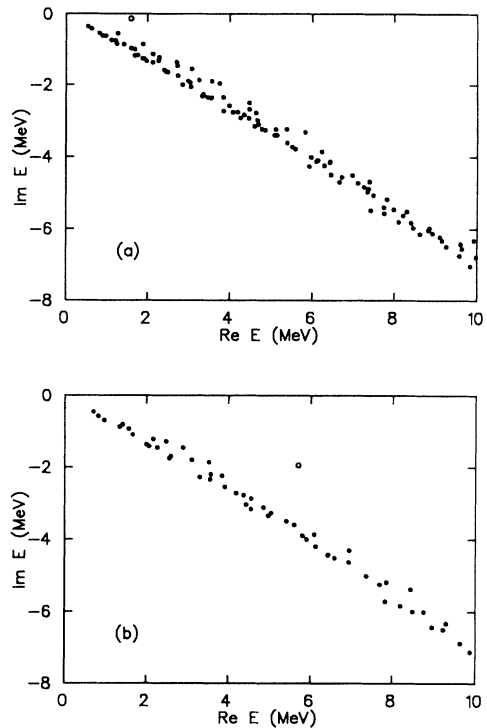


FIG. 1. Energy eigenvalues of the complex scaled Hamiltonian of the (a)  $2^+$  and (b)  $1^+$  states of  ${}^6\text{Li}$ . The dots are the points of the rotated discretized continua, while the circles are three-body resonances. The rotation angle is 0.3 rad.

picture a bit fuzzy, but the identification of the resonant states is unambiguous.

In Fig. 2 we show our result for the  $1^-$  state of  ${}^6\text{He}$ , where the soft dipole mode was predicted at  $(6 - i2.5)$  MeV ( $E = 6$  MeV,  $\Gamma = 5$  MeV [9]). As we can see, our model does not confirm the existence of such a state. No resonant state occurred while increasing the  $\theta$  value to as large as 0.7, where the CSM becomes unstable. This result is in agreement with [35,36], where the authors did not find any indication for the existence of a  $1^-$  state,

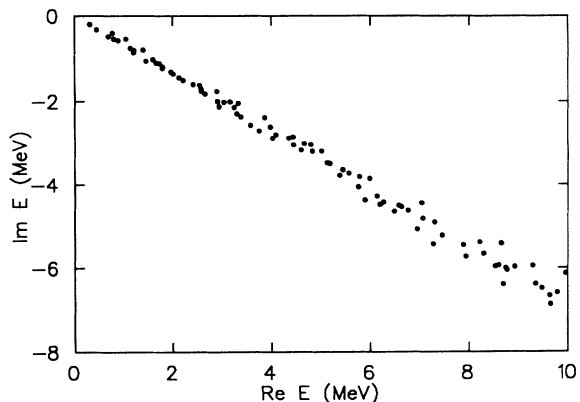


FIG. 2. Energy eigenvalues of the complex scaled Hamiltonian of the  $1^-$  states of  ${}^6\text{He}$ . The rotation angle is 0.3 rad.

analyzing the  ${}^6\text{He}$  strength functions and break-up cross sections at real energies.

In the literature there are works for the  $A = 6$  nuclei in which the three-body resonance parameters are extracted from real energy phase shifts [19,37], and Faddeev calculations [20–22], respectively. The results of these works are consistent with each other and with ours, except that in [37], in addition to the well-known  $0^+$  ground state and  $2^+$  excited state, the authors found low-lying narrow  $0^+$  and  $1^+$  excited states in  ${}^6\text{Be}$ , a fact which we try to explain later.

In [12] we argued that we can identify three-body resonances using the fact that they have to appear in each possible Jacobi coordinate system. Here, using the  $2^+$  state of  ${}^6\text{He}$ , we check this claim. Switching off all  $\alpha(nn)$  and  $n(\alpha n)$  channels, respectively, the resonance occurs at  $1.01 - i0.081$  MeV and  $1.89 - i0.094$  MeV, respectively. If we keep only the  $(S, L) = (0, 2)$  channels, we get the resonance at  $2.00 - i0.446$  MeV, while keeping only the  $(S, L) = (1, 1)$  configurations the resonance appears at  $2.04 - i0.760$  MeV. Thus, our present model shows that the three-body resonances appear not just in every different Jacobi coordinate systems, but in every different  $(S, L)$  configuration. It means that a  $1^-$  three-body resonance, if it exists, must show up even if our model space were very restrictive.

To sum up our results, we have found the experimentally known resonances, but not found any indication that the  $1^-$  soft dipole mode exists in  ${}^6\text{He}$ . In the next section we give a possible explanation of the experimental finding of soft dipole resonances in neutron halo nuclei.

#### IV. DISCUSSION

We have shown in [12] that if there are resonances in a two-body subsystem of a three-body system, then the sequential decay of the system through these resonant states leads to structures in the three-body continuum, in addition to the structures coming from the three-body resonances. This is because around the two-body resonance energy, in addition to the three-body phase space, a substantial two-body phase space is available for the system to decay into. We emphasize that these structures have kinematical, rather than dynamical origin. The  $0^+$  and  $1^+$  excited states of  ${}^6\text{Be}$ , found in [37], are nice examples to demonstrate the operation of the sequential decay mode. The model wave function of [37] consists of  ${}^3\text{He}+{}^3\text{He}$  and  ${}^5\text{Li}+p$  channels with, bound state approximated,  $3/2^-$ ,  $1/2^-$ , and  $3/2^+$   ${}^5\text{Li}$  states. The  $0^+$  and  $1^+$  resonances of [37] in the  ${}^6\text{Be}$  phase shifts are apparent. They are the consequence of the fact that the  ${}^5\text{Li}+p$  asymptotic decay modes are built into the wave function. These states are sequential decay modes, having two-body dynamical structures. Thus, these are not three-body resonances in  ${}^6\text{Be}$ . In a similar work [19] the method of the hyperspherical harmonics does not allow sequential decay modes, that is why the authors did not find excited  $0^+$  and  $1^+$  in the  ${}^6\text{Be}$  phase shifts.

We can conclude from our results that it is possible that the soft dipole mode does not exist in  ${}^6\text{He}$ , and the

experiments see only the  ${}^5\text{He}+n$  sequential decay mode of this nucleus. We show that there is no experimental finding which contradicts our assumption.

In  ${}^6\text{He}$  the sequential decay mode leads to a superposition of the  $3/2^-$  and  $1/2^-$   ${}^5\text{He}$  states and the neutron in the final state. The angular momentum of the relative motion is most probably  $l = 0$  to avoid the centrifugal barrier. As a consequence,  $0^-$ ,  $1^-$ , and  $2^-$  structures can appear in the excitation function of  ${}^6\text{He}$ . From the  $0^+$  ground state, only the  $1^-$  state can be excited conventionally, the other two states can only be excited by parity transfer e.g. by using pions. Due to the splitting of the  $3/2^-$  and  $1/2^-$  states of  ${}^5\text{He}$  (these states are at 0.89 MeV and 4 MeV [32], respectively), two  $1^-$  bumps can appear in the excitation function of  ${}^6\text{He}$  at  $0.975+0.89 \approx 1.9$  MeV and  $0.975+4 \approx 5$  MeV excitation energies, respectively (0.975 MeV is the two-neutron separation energy of  ${}^6\text{He}$ ). In recent experiments [9,10] a  $1^-$  structure appeared around 6 MeV, and the well-known  $2^+$  state at 1.8 MeV. The position of the  $1^-$  bump is in good agreement with our prediction, while our other structure at 1.9 MeV coincides with the position of the  $2^+$  state. We can see in Fig. 2 of [9] that the assumption of a mixed  $2^+$  and  $1^-$  nature of the bump at 1.8 MeV is not in contradiction with the measured angular distribution, on the contrary, it would improve the agreement between theory and experiment.

Let us point out that a similar situation may occur in  ${}^{11}\text{Li}$ . Here the sequential decay mode leads to  ${}^{10}\text{Li}+n$  final states. There are several measurements for the low-lying resonances of  ${}^{10}\text{Li}$  (see, e.g., [38]), the most recent Ref. [39], which seems to be the most reliable, gives a  $1^+$  state at 0.42 MeV, and a  $2^+$  state at 0.8 MeV excitation energies. The most recent value of the two-neutron separation energy of  ${}^{11}\text{Li}$  is  $0.295 \pm 0.035$  MeV [40]. The sequential decay mode can lead to structures around  $0.42+0.29 \approx 0.7$  and  $0.8+0.29 \approx 1.1$  MeV  ${}^{11}\text{Li}$  excitation energies. Assuming again that the  $l = 0$  angular momentum between  ${}^{10}\text{Li}$  and  $n$  is preferred, the possible  $J^\pi$  values are  $1/2^+$  and  $3/2^+$  at 0.7 MeV, and  $1/2^+$ ,  $3/2^+$ , and  $5/2^+$  at 1.1 MeV. All of these  $J^\pi$  states can be excited from the  $3/2^-$  ground state of  ${}^{11}\text{Li}$  without parity transfer, which means that the experimental structure is a coherent superposition of them. In [2,8] a bump occurred in the  ${}^{11}\text{Li}$  excitation spectrum around 1.2 MeV excitation energy. The position and the experimentally observed  $1/2^+$ ,  $3/2^+$ , or  $5/2^+$  spin-parity character of this state are again in good agreement with our result. In [39] a state in  ${}^{10}\text{Li}$  is also found around 4 MeV, and in [2,8] we can see some structures in this energy region, too.

In Ref. [41] the authors studied the Coulomb break-up of  ${}^{11}\text{Li}$  on Pb target. They found that the average velocity of the outgoing  ${}^9\text{Li}$  nuclei is larger than the average velocity of the outgoing neutrons. They explained this by the post acceleration of the  ${}^9\text{Li}$  nuclei in the field of the lead target nucleus. From the large velocity shift they concluded that the breakup process should be direct, not resonant through the presumed soft dipole mode. If the sequential decay mode causes the apparent resonancelike structure in  ${}^{11}\text{Li}$ , as we assume, then the

post acceleration is felt by the  $^{10}\text{Li}$  particle (and not by the other neutron), thus the average neutron velocity can be smaller than that of the  $^9\text{Li}$  velocity. In Fig. 14 of [41] one can see two peaks of the velocity shift curve. The larger shift is probably due to the direct breakup (the three-body scattering final state), while the other peak at much smaller shift can account for the sequential decay.

The complete kinematical measurement of [41] would allow a stringent test of our assumption that there is no soft dipole mode in  $^{11}\text{Li}$ , only a sequential decay mode. In the center-of-mass frame one should see a considerable increase of the  $180^\circ$  angular correlation between  $^9\text{Li}$  and neutrons around the 1.2 MeV excitation of  $^{11}\text{Li}$ .

## V. CONCLUSIONS

In summary, we have searched for low-energy three-body resonances in  $^6\text{He}$ ,  $^6\text{Li}$ , and  $^6\text{Be}$ , using the complex scaling method in a microscopic three-cluster model. Our model can account both for the correct nuclear physics and the proper three-body dynamics. However, due to the fact that our interaction is not fully adequate in the triplet-even partial wave, our description of  $^6\text{Li}$  can only be considered as a test case. We have found the experimentally known resonances, except a  $2^+$  state of  $^6\text{Li}$ , which cannot be localized by our present method. However, we have not found the predicted  $1^-$  soft dipole mode

in  $^6\text{He}$ . We argued that this state, if it exists, should appear even in a model which is much simpler than ours.

We concluded from our result that it is possible that the soft dipole modes of the neutron halo nuclei do not exist, and the experiments see just the sequential decay modes of these nuclei. We have shown, through the examples of  $^6\text{He}$  and  $^{11}\text{Li}$ , that there is no experimental fact which contradicts this assumption. A test of our assumption could come from the analysis of the experimental core-neutron angular correlation in breakup reactions. If the sequential decay mode has a significant effect, then a strong increase of the  $180^\circ$  correlation in the center-of-mass frame should be found around the “resonance” energies.

Finally, we mention that the importance of the sequential decay modes was pointed out in [42], claiming that the broad part of the momentum distribution of the projectile fragments in the neutron halo nuclei probably comes from these modes.

## ACKNOWLEDGMENTS

This work was supported by the Fulbright Foundation and NSF Grant Nos. PHY90-13248 and PHY91-15574 (USA), and by OTKA Grant Nos. 3010 and F4348 (Hungary). I wish to thank S. E. Koonin and K. Langanke for useful comments on the manuscript.

- 
- [1] I. Tanihata, Nucl. Phys. **A553**, 361c (1993).
  - [2] T. Kobayashi, Nucl. Phys. **A538**, 343c (1992).
  - [3] T. Kobayashi, Nucl. Phys. **A553**, 465c (1993).
  - [4] P. G. Hansen, Nucl. Phys. **A553**, 89c (1993).
  - [5] *Proceedings of the International Symposium on Structure and Reactions of Unstable Nuclei*, Niigata, Japan, 1991, edited by K. Ikeda and Y. Suzuki (World Scientific, Singapore, 1991).
  - [6] P. G. Hansen and B. Jonson, Europhys. Lett. **4**, 409 (1987); K. Ikeda, in [5], p. 3; Y. Suzuki and K. Ikeda, Phys. Rev. C **38**, 410 (1988).
  - [7] N. Poppelier, L. Wood, and P. Glaudemans, Phys. Lett. **157B**, 120 (1985); Y. Suzuki and Y. Toshaka, Nucl. Phys. **A517**, 599 (1990); A. C. Hayes and D. Strottman, Phys. Rev. C **42**, 2248 (1990).
  - [8] T. Kobayashi, in [5], p. 187.
  - [9] S. B. Sakuta, A. A. Ogloblin, O. Ya. Osadchy, Yu. A. Glukhov, S. N. Ershov, F. A. Gareev, and J. S. Vaagen, Europhys. Lett. **22**, 511 (1993).
  - [10] F. Brady, G. A. Needham, J. L. Romero, C. M. Castaneda, T. D. Ford, J. L. Ullmann, and M. L. Webb, Phys. Rev. Lett. **51**, 1320 (1983).
  - [11] Y. Suzuki, Nucl. Phys. **A528**, 395 (1991).
  - [12] A. Csóto, Phys. Rev. C **49**, 2244 (1994).
  - [13] A. Csóto, Phys. Rev. C **48**, 165 (1993).
  - [14] D. R. Thompson, M. LeMere, and Y. C. Tang, Nucl. Phys. **A268**, 53 (1977); I. Reichstein and Y. C. Tang, *ibid.* **A158**, 529 (1970).
  - [15] A. Csóto and D. Baye, Phys. Rev. C **49**, 818 (1994).
  - [16] P. Heiss and H. H. Hackenbroich, Phys. Lett. **30B**, 373 (1969).
  - [17] A. Csóto, R. G. Lovas, and A. T. Kruppa, Phys. Rev. Lett. **70**, 1389 (1993).
  - [18] N. W. Schellingerhout, L. P. Kok, S. A. Coon, and R. M. Adam, Phys. Rev. C **48**, 2714 (1993).
  - [19] B. V. Danilin and M. V. Zhukov, Yad. Fiz. **56**, 67 (1993) [Sov. J. Nucl. Phys. **56**, 460 (1993)].
  - [20] Y. Matsui, Phys. Rev. C **22**, 2591 (1980).
  - [21] A. Eskandarian and I. R. Afnan, Phys. Rev. C **46**, 2344 (1992).
  - [22] V. G. Emelyanov, V. I. Klimov, and V. N. Pomerantsev, Phys. Lett. **157B**, 105 (1985).
  - [23] Y. K. Ho, Phys. Rep. **99**, 1 (1983); N. Moiseyev, P. R. Certain, and F. Weinhold, Mol. Phys. **36**, 1613 (1978); Proceedings of the Sanibel Workshop Complex Scaling, 1978 [Int. J. Quantum Chem. **14**, 343 (1978)]; B. R. Junker, Adv. At. Mol. Phys. **18**, 207 (1982); W. P. Reinhardt, Annu. Rev. Phys. Chem. **33**, 223 (1982); *Resonances—The Unifying Route Towards the Formulation of Dynamical Processes, Foundations and Applications in Nuclear, Atomic and Molecular Physics*, edited by E. Brändas and N. Elander, Lecture Notes in Physics Vol. 325 (Springer-Verlag, Berlin, 1989).
  - [24] M. Reed and B. Simon, *Methods of Modern Mathematical Physics* (Academic Press, New York, 1978).
  - [25] J. Aguilar and J. M. Combes, Commun. Math. Phys. **22**, 269 (1971); E. Balslev and J. M. Combes, *ibid.* **22**, 280 (1971); B. Simon, *ibid.* **27**, 1 (1972).

- [26] A. T. Kruppa, R. G. Lovas, and B. Gyarmati, *Phys. Rev. C* **37**, 383 (1988).
- [27] A. T. Kruppa and K. Katō, *Prog. Theor. Phys.* **84**, 1145 (1990).
- [28] K. Katō and K. Ikeda, *Prog. Theor. Phys.* **89**, 623 (1993).
- [29] H. Kameyama, M. Kamimura, and M. Kawai, in [5], p. 203.
- [30] R. Beck, F. Dickmann, and R. G. Lovas, *Ann. Phys. (N. Y.)* **173**, 1 (1987).
- [31] A. Csótó and R. G. Lovas, *Phys. Rev. C* **46**, 576 (1992).
- [32] F. Ajzenberg-Selove, *Nucl. Phys.* **A490**, 1 (1988).
- [33] A. Csótó, *Phys. Rev. A* **48**, 3390 (1993).
- [34] I. R. Afnan, *Aust. J. Phys.* **44**, 201 (1991).
- [35] B. V. Danilin, M. V. Zhukov, J. S. Vaagen, and J. M. Bang, *Phys. Lett. B* **302**, 129 (1993).
- [36] L. S. Ferreira, E. Maglione, J. M. Bang, I. J. Thompson, B. V. Danilin, M. V. Zhukov, and J. S. Vaagen, *Phys. Lett. B* **316**, 23 (1993).
- [37] H. M. Hofmann and W. Zahn, *Nucl. Phys.* **A368**, 29 (1981).
- [38] K. H. Wilcox, R. B. Weisenmiller, G. J. Wozniak, N. A. Jelley, D. Ashery, and J. Cerny, *Phys. Lett.* **59B**, 142 (1975); A. I. Amelin, M. G. Gornov, Yu. B. Gurov, A. L. Ilin, P. V. Morokhov, V. A. Pechkurov, V. I. Savelev, F. M. Sergeev, S. A. Smirnov, B. A. Chernyshev, R. R. Shafigullin, and A. V. Shishkov, *Yad. Fiz.* **52**, 1231 (1990) [*Sov. J. Nucl. Phys.* **52**, 782 (1990)].
- [39] H. G. Bohlen, B. Gebauer, M. von Lucke-Petsch, W. von Oertzen, A. N. Ostrowski, M. Wilpert, Th. Wilpert, H. Lenske, D. V. Alexandrov, A. S. Demyanova, E. Nikolskii, A. A. Korshennikov, A. A. Ogloblin, R. Kalpakchieva, Y. E. Penionzhkevich, and S. Piskor, *Z. Phys. A* **344**, 381 (1993).
- [40] B. M. Young, W. Benenson, M. Fauerbach, J. H. Kelley, R. Pfaff, B. M. Sherrill, M. Steiner, J. S. Winfield, T. Kubo, M. Hellström, N. A. Orr, J. Stetson, J. A. Winger, and S. J. Yennello, *Phys. Rev. Lett.* **71**, 4124 (1993).
- [41] D. Sackett, K. Ieki, A. Galonsky, C. A. Bertulani, H. Esbensen, J. J. Kruse, W. G. Lynch, D. J. Morrissey, N. A. Orr, B. M. Sherrill, H. Schulz, A. Sustich, J. A. Winger, F. Deák, Á. Horváth, Á. Kiss, Z. Seres, J. J. Kolata, R. E. Warner, and D. L. Humphrey, *Phys. Rev. C* **48**, 118 (1993).
- [42] I. Tanihata, in [5], p. 233.